Available online at www.sciencedirect.com

ScienceDirect

Catalysis Today 122 (2007) 178–185

CATALYSIS TODAY

www.elsevier.com/locate/cattod

Photocatalytic oxidation of 1,1-dimethyl hydrazine vapours on TiO_2: FTIR *in situ* studies

P.A. Kolinko [a,*], D.V. Kozlov [a,*], A.V. Vorontsov [a], S.V. Preis [b]

[a] *Boreskov Institute of Catalysis, Novosibirsk 630090, Russia*
[b] *Lappeenranta University of Technology, Lappeenranta 53850, Finland*

Abstract

Gas phase photocatalytic oxidation (PCO) of unsymmetrical dimethyl hydrazine (UDMH) in a batch reactor using TiO_2 as the photocatalyst was studied with *in situ* FTIR method. Carbon dioxide, water, nitric acid and nitrogen were detected as the ultimate PCO products of UDMH. Adsorbed N_2O species were detected as the main surface intermediates. The formation of the extremely toxic intermediate, nitrosodimethylamine $(CH_3)_2NNO$, was not observed. The reaction mechanism based on detected products distribution, kinetics analysis and previously published data is discussed.

Long-term experiments were carried out to determine the photocatalyst stability in PCO of UDMH: the catalyst exhibited stable performance; the rate of deactivation was low due to transformation of nitrogen mainly to N_2. Only 10% of UDMH nitrogen was transformed to HNO_3 in adsorbed form.

Keywords: Rocket propellant; Air purification; Adsorption; UDMH; Nitrosodimethylamine

1. Introduction

Unsymmetrical dimethylhydrazine (1,1-dimethylhydrazine, UDMH) is a widely used rocket propellant and an extremely toxic compound [1].

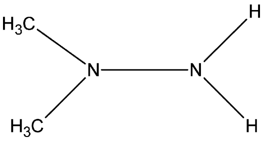

The development of methods of UDMH removal from water and air is an urgent task for substantial stocks to be handled, stored and utilized on the course of disarmament. The method currently known for the UDMH stocks abatement is a catalytic incineration [2], which is not appropriate for the treatment of water and air containing UDMH as a pollutant. Oxidation with ozone, catalytic oxidation with oxygen and hydrogen peroxide in the presence of Cu, Fe, Co salts supported on zeolites as catalysts [3,4] and oxidation with chloramine [5,6] may be used for the removal of UDMH from water. However, the main disadvantage of these methods is formation of *N*-nitrosodimethylamine $(CH_3)_2N–N=O$ (NDMA) as an intermediate of UDMH oxidation, which is even more toxic than UDMH [7,8].

Unsymmetrical dimethyl hydrazine is highly volatile substance, the vapour pressure is 13.7 kPa at 20 °C [9]. This makes UDMH concentrations in propellant storage and utilization sites' air often exceeding the maximum permissible concentration of 0.1 mg/m^3 [10].

Photocatalytic oxidation (PCO) over near-UV ($\lambda < 360$ nm) irradiated titanium dioxide is considered to be an advantageous method for the removal of UDMH vapours for the high oxidative potential of the titanium dioxide surface (about +3 V versus SHE) [11], which makes the majority of organic compounds oxidizible to ultimate inorganic compounds avoiding hazardous by-products.

The present work deals with the kinetics of the gas phase PCO of UDMH in a batch reactor, the catalyst activity in a long-term use, and the identification of the gas phase and surface intermediates, establishing the UDMH PCO reaction pathways by the FTIR *in situ* method. Two lamps were used for these tasks. The mobile high pressure Hg lamp was used for

---

* Corresponding authors. Tel.: +7 383 3331617.
E-mail addresses: kolinko@catalysis.ru (P.A. Kolinko), kdv@catalysis.ru (D.V. Kozlov).

0920-5861/$ – see front matter © 2007 Published by Elsevier B.V.
doi:10.1016/j.cattod.2007.01.029

conducting *in situ* FTIR experiments and the stationary high pressure Xe lamp was used for batch reactor experiments.

2. Experimental

2.1. Materials

Unsymmetrical dimethyl hydrazine used in all experiments was taken as a rocket propellant from the military rocket base near to Novosibirsk. The content of UDMH was determined by the KIO_3 titration method for the UDMH solutions of high concentrations according to Malone and Anderson [12]. The UDMH concentration in the rocket propellant was determined as $C_0 = 94 \pm 2$ wt.% and the remaining part consists of water. Distilled water purified with Barnstead "Easy pure II" ultra pure water system ($r = 18.2\ \mathrm{M\Omega\ cm^{-1}}$) was used in all experiments. Titanium dioxide, Sachtleben Chemie GmbH, 100% anatase, S_{BET} 347 m^2/g, average pore diameter 4.9 nm, was used as the photocatalyst in this work.

2.2. FTIR in situ experiments

For the analysis of the gas phase products and the detection of surface intermediates during the UDMH PCO, the FTIR *in situ* method was employed. To prepare TiO_2 samples, 200 μL of the aqueous suspension containing 15.7 mg ml^{-1} of TiO_2 sonicated in an ultrasonic bath for 15 min were uniformly deposited onto a CaF_2 support plate with the diameter of 20 mm and thickness of 1 mm and dried at room temperature. This made the TiO_2 density on the obtained samples equal to about 1 mg cm^{-2}. These samples were placed in a 300 cm^3 IR cell (Fig. 1), which was installed in the IR Spectrometer Vector 22 (Bruker) cell compartment. The main specific feature of the cell construction used in our experiments is the ability of placing the TiO_2 sample in or out of the IR beam without disturbing the reaction gas mixture in the cell. In this way, one could measure IR spectra of either the gas phase or the TiO_2 catalyst surface with adsorbed species without opening the cell. Each IR spectrum was averaged from 32 scans in the 1000–4000 cm^{-1} wave number region with the 2 cm^{-1} resolution.

The high pressure Hg lamp DRSh-1000 (Russia) was used as the UV light source. Samples were irradiated by condensed light passing through a water filter to cut-off infrared radiation, having major spectrum line at 365 nm (20 mW/cm^2).

The measurement of light intensity was conducted by the microvolt meter F-136 (Russia) equipped with the semiconductor light intensity detector calibrated with the actinometer.

2.3. Batch reactor kinetics

For the photocatalyst life time and products' analysis, the batch 434-cm^3 reactor equipped with a quartz cover for the sample illumination was used. The TiO_2 sample preparation was similar to the FTIR *in situ* experiments with the exception that the glass plate support was used instead of CaF_2 (Fig. 2). The mass of TiO_2 catalyst was 3.14 mg at the irradiated area of 3.14 cm^2. All geometrical surface TiO_2 has been irradiated in the IR cell and the batch reactor. An air flow of 300 cm^3 min^{-1} of required humidity passed through the reactor with the TiO_2 sample placed inside for 1 h before the experiment for equalizing the humidity of the air and the sample. After that, 0.5 μl of UDMH was injected into the reactor and the reactor was left for 20 min for the adsorption equilibrium to be established.

The irradiation of the sample was conducted by means of a high pressure Xe lamp equipped with the water filter and the band pass interference filter (λ_{max} 334 nm). The incident light intensity was equal to 5.8 mW cm^{-2}.

The analysis of gaseous samples from the static reactor taken at 10 min time intervals was performed on a gas chromatograph LHM-8 (Russia) equipped with a flame-ionization detector.

The measurements of the final nitrogen-containing inorganic products of PCO residing over the TiO_2 surface were carried out with the ion meter "I-130 M" (Russia) equipped with the NH_4^+ and NO_3^- preliminarily calibrated ion selective electrodes in rinsing water. For these measurements, the TiO_2 powder was transferred from the glass support to a beaker with 20 ml of rinsing water added.

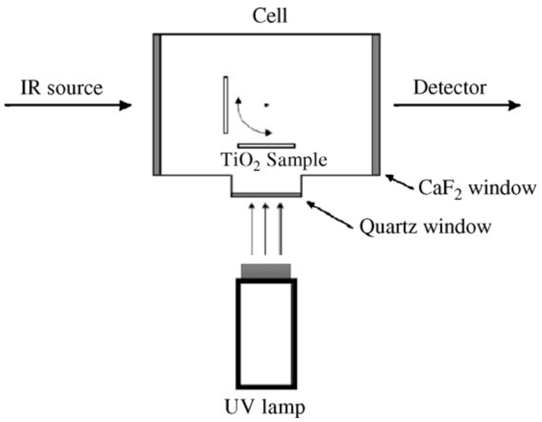

Fig. 1. The schematic diagram of top view of the *in situ* FTIR experimental setup. Optical path of the cell 10 cm, cell volume 300 ml.

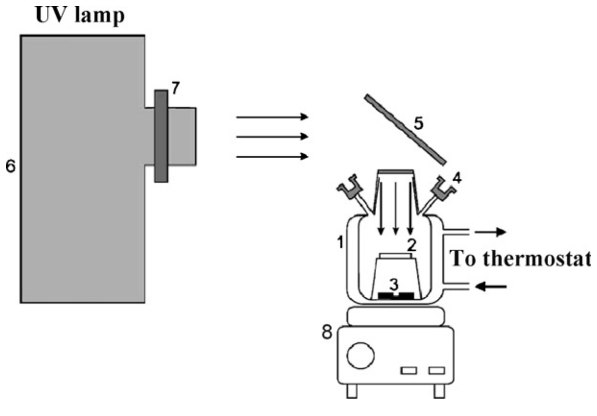

Fig. 2. An external view of the batch reactor setup: 1, batch reactor; 2, TiO_2 sample; 3, stir bar; 4, sampling port; 5, mirror; 6, light source; 7, condenser with light filter; 8, magnetic stirrer.

3. Results and discussion

3.1. FTIR study

After injected into the IR cell UDMH evaporated and its adsorption on the catalyst surface completed, the UV was allowed to irradiate the photocatalyst surface. The IR spectra of the gas phase and the TiO_2 surface were periodically taken for PCO results monitoring. The results of the UDMH and CO_2 evolutions during the PCO experiment are shown in Fig. 3. Both concentrations of UDMH and CO_2 were calculated from the areas of the corresponding IR spectra bands using integral form of Lambert's absorption law[1] and factors of integrated absorption $A_{02775\,\mathrm{cm}^{-1}} = 1.158 \times 10^{-5}\,\mathrm{ppm}^{-1}\,\mathrm{cm}^{-2}$ и $A_{02280-2400\,\mathrm{cm}^{-1}} = 7.5 \times 10^{-4}\,\mathrm{ppm}^{-1}\,\mathrm{cm}^{-2}$ for UDMH and CO_2, respectively.

One can see from Fig. 3 that a major part of UDMH adsorbed on the TiO_2 surface for the time of the irradiation start: the inserted concentration of 538 ppm decreased with the adsorption to 126 ppm About 85% of initial UDMH carbon transformed to the CO_2 after 80 min of irradiation. The residues remained on the TiO_2 surface in the form of adsorbed carbonates with IR absorption bands ν_{as}(COO) 1260 cm^{-1} and ν_s(C=O) 1583 cm^{-1} [13]. This assumption also was proved by the TOC analysis of the rinsing water after the end of the experiment: the rinsing water contained about 15% of initial organic carbon.

Quantum efficiency (amount of quanta of light used for oxidation) was calculated according to the formula $\varphi = n(W/IS)$, in which W is the speed of oxidation of the UDMH (molecules/c), I the intensity of light (quanta/cm^2), S the illuminated area of a sample (cm^2), n the amount of charges carriers (holes) participating in oxidation of one molecule of a substratum for the case of UDMH $n = 16$. In our experiments all the geometric surface of the sample (3.14 cm^2) was illuminated.

$$H_2^{+1}N^{-2} - N^{-2}(C^{-2}H_3^{+1})_2 + 4O_2 \xrightarrow{TiO_2,h\nu} 2C^{+4}O_2 + N_2^0 + 4H_2O \qquad (X)$$

The origin of the number $n = 16$ is based upon the following:

1. The N_2 is the main N-containing product of the UDMH PCO (see the Section 3.2 of the "Result and discussion");
2. The gross equation of the UDMH PCO is close to the Eq. (X);
3. The total change of oxidation numbers of carbon and nitrogen atoms in this equation is equal to 16 = +8 (after) − (−8) (before);
4. The every change of oxidation number by the value of 1 requires one electron-hole pair and therefore one quantum of absorbed UV light;
5. The CO_2 accumulation rate is two times higher than the UDMH oxidation rate.

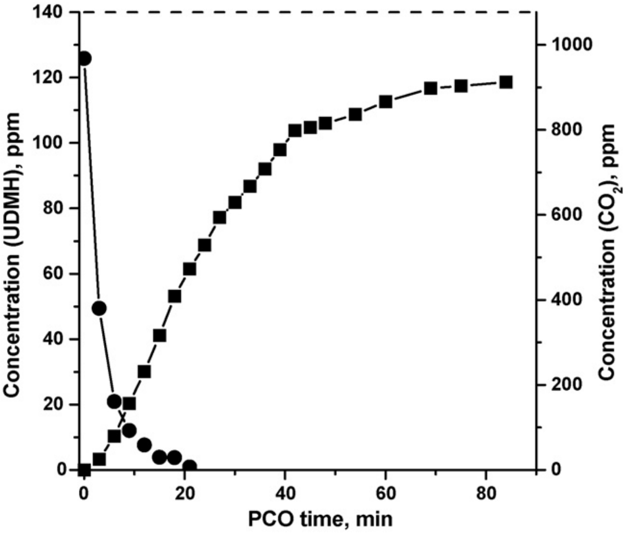

Fig. 3. CO_2 accumulation (■) and UDMH vapour removal (●) in PCO of 0.5 μl UDMH in the IR cell: 300 K, relative humidity 0%. Dashed line corresponds to the theoretical 100% UDMH conversion to gaseous CO_2.

The 4th assumption is rough because we know that some stages of the complicated reactions could be run in the dark without charge carriers participation. So we suppose that the quantum efficiency calculated according to our approach is lower than the real value.

The 5th assumption is based upon the fact that one UDMH molecule contains two carbon atoms and during the long time experiment when the conversion is close to 80–100% the average rate of CO_2 accumulation is two times higher than the UDMH PCO rate.

Quantum efficiency φ of the UDMH PCO during the first 30 min equalled to 18.6%, which was calculated from the assumption that all quanta are of 365 nm wavelength.

The IR spectra of the gas phase and the TiO_2 photocatalyst surface during UDMH PCO are shown in Fig. 4. Analysis of these spectra reveals that:

- almost all UDMH disappears from the TiO_2 surface after 40 min of PCO (absorption bands 2785, 2831, 2865 and 2964 cm^{-1} attributed to symmetric and asymmetric valence vibrations of C–H bond in UDMH disappear [14]);
- nitric acid forms as the final product of UDMH PCO on the TiO_2 surface seen as 1308 and 1436 cm^{-1} broad bands on spectrum 4 (Fig. 4B) compared with the IR spectrum of HNO_3 adsorbed on TiO_2 surface (Fig. 5);
- at least one surface intermediate forms during PCO of UDMH. Adsorption band at 2206 cm^{-1} appeared immediately after the start of illumination, reached its maximum in 40 min (spectrum 2, Fig. 4B) and completely disappeared at the end of PCO.

The adsorption band at 2206 cm^{-1} was attributed to the absorbed N_2O species for the following reasons:

- the formation of the same surface intermediate with 2206 cm^{-1} absorption band was observed during the PCO

---

[1] $A = A_0Cl$, where A is the area of an absorption band (cm^{-1}), l the optical pathlength (cm), C the gas concentration (ppm) and A_0 is the aspect ratio (ppm^{-1} cm^{-2}).

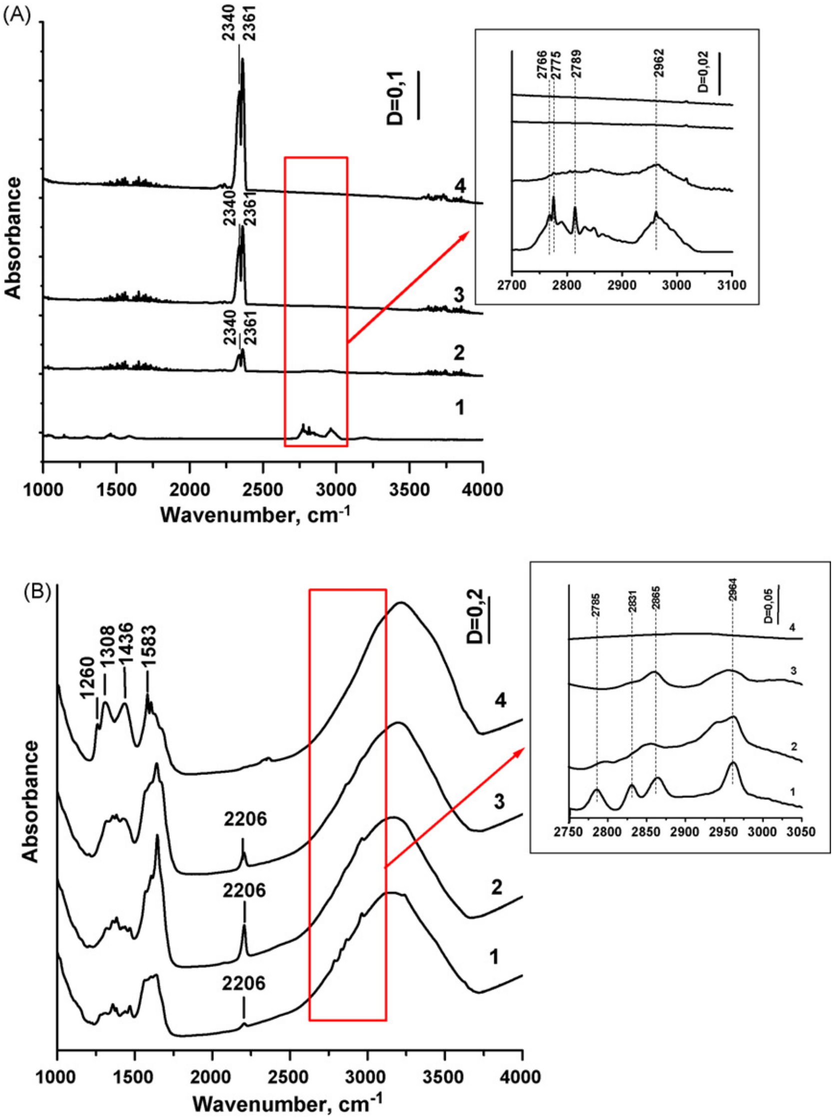

Fig. 4. FTIR spectra of the gas phase (A) and the TiO_2 surface (B) in PCO of 0.5 μl UDMH in the IR cell: 300 K, relative humidity 0%. Numbers of curves correspond to irradiation time 1–2 min; 2–10 min; 3–40 min and 4–120 min. D – Absorbance. On the zoom area (Fig. B) there were subtracted the straight line from all the spectra for the convenient view.

of UDMH, NDMA and hydrazine (see Fig. 6, spectra 4, 3 and 2 respectively);

- a small amount of gaseous N_2O was detected in the IR cell after the end of PCO of all the three species (UDMH, NDMA and hydrazine);
- the N–N absorption band of gaseous N_2O (2206 cm^{-1}) is close to that observed for the surface intermediate (see Fig. 6, spectrum 1).

3.2. The analysis of N-containing products

We demonstrated in our previous study of gas phase PCO of diethyl sulphide that the photocatalyst deactivation takes place due to accumulation of surface sulphates [15]. In the present work we also studied the problem of TiO_2 deactivation with the UDMH PCO products. The first question under consideration was the distribution of ultimate nitrogen-containing PCO products, which could be divided into two groups (see Table 1).

Nitrosodimethylamine was detected among neither intermediates, nor end PCO products of UDMH with GC/MS analysis of rinsing water from the TiO_2 surface. Also, the analysis of FTIR spectra of the gas phase during PCO experiments and their correlation with NDMA FTIR spectra published by the other authors did not indicate any presence of NDMA [16].

The analysis of the ultimate N-containing species adsorbed on TiO_2 samples was conducted using ion-selective electrodes for NH_4^+ and NO_3^- in the rinsing water resulted from a complete (3 h) PCO of a small amount of UDMH (0.5 μl) at 3 mg TiO_2 sample. The amount of evolved N_2 was estimated as the difference between the initial amount of UDMH and the sum of NH_4^+ and NO_3^-. The results are presented in Table 2. The majority of UDMH nitrogen transforms to the molecular N_2, ammonia being present in a very small amount. The predominant formation of molecular nitrogen as the final product is important from the practical point of view, allowing

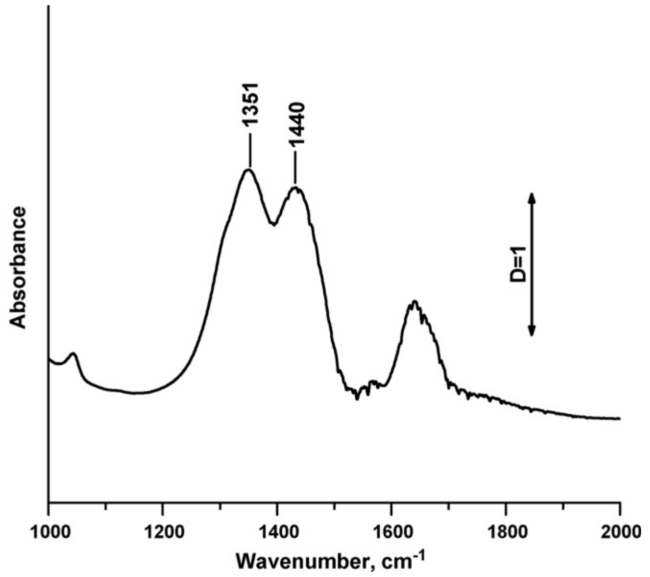

Fig. 5. IR spectrum of HNO_3 adsorbed on the TiO_2 surface. D – Absorbance.

application of PCO for effective degradation of hydrazines without formation of secondary pollutants, nitrogen oxides.

3.3. PCO pathways for UDMH and other hydrazines

The formation of surface nitrates and ammonia was observed as a result of PCO of hydrazine (N_2H_4) and NDMA, similarly to UDMH. Similar PCO behaviour of all three species – formation of common intermediates $N_2O_{(ads)}$ and $N_2O_{(gas)}$ and also end products NH_4^+, NO_3^- and N_2, the following reaction rationale of PCO could be proposed:

$$TiO_2 + h\nu \rightarrow h^+ + e^- \quad (1.0)$$

$$h^+ + H_2O_{(ads)} \rightarrow \dot{O}H_{(ads)} + H^+ \quad (1.1)$$

$$O_{2(gas)} \rightarrow O_{2(ads)} \quad (1.2)$$

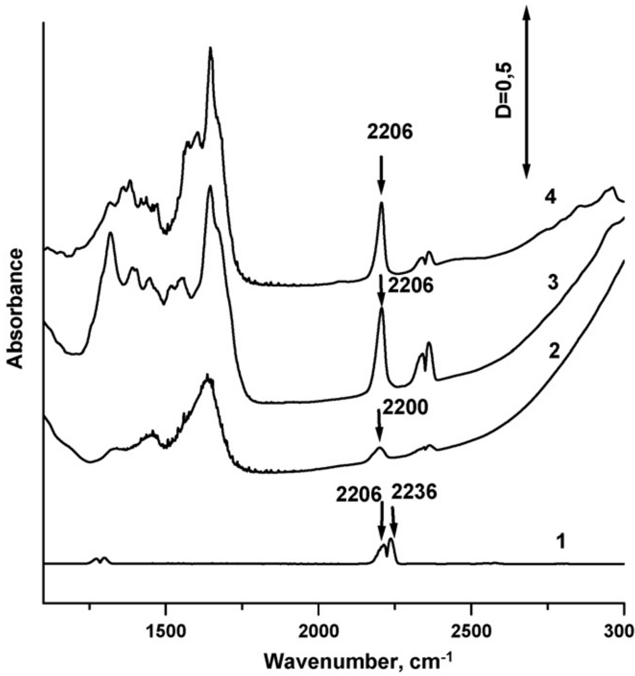

Fig. 6. IR spectra of the TiO_2 surface in 10 min of PCO of (2) – hydrazine (N_2H_4), (3) – nitrosodimethylamine ($(CH_3)_2N{-}N{=}O$) and (4) – 1,1-dimethylhydrazine ($(CH_3)_2N{-}NH_2$), 1 – the IR spectrum of gaseous N_2O. D – Absorbance.

$$O_{2(ads)} \rightarrow 2O_{(ads)} \quad (1.3)$$

$$e^- + O_{2(ads)} \rightarrow O^-_{2(ads)} \quad (1.4)$$

$$e^- + O_{(ads)} \rightarrow O^-_{(ads)} \quad (1.5)$$

Stages (1.0)–(1.5) are common for the photocatalytic oxidation of all three substrates and describe the formation of active particles ($\dot{O}H$, O^- and O_2^-) on the TiO_2 surface under the UV radiation [17,18].

The next stages describe the adsorption of N_2H_4 on the TiO_2 surface leading to the breakage of N–N bond (2.1) [19] and the

Table 1
N-containing products of UDMH PCO

Product	Gaseous form	Adsorbed form	Detection method
Intermediates			
Nitrosodimethylamine	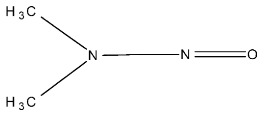	—	Was not detected
Nitrogen (I) oxide	N_2O	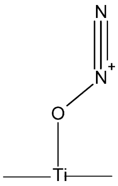	Surface FTIR spectra, PM3 simulation
Final products			
Ammonia	NH_3	NH_4^+	Water washout analysis by ion selective electrodes
Nitric acid	HNO_3	NO_3^-	
Nitrogen	N_2	—	Calculated from nitrogen balance

Table 2
Mole fraction of N-containing PCO products of UDMH, NDMA, N_2H_4, and NH_3 after 180 min irradiation (temperature $T = 300$ K, humidity $\chi = 0\%$, illumination was conducted by condensed light of high pressure Hg lamp, $W = 20$ mW/cm^2)

Substance	Mole fraction of the products of PCO (ω), %			
	N_2	N_2O	NH_4^+	NO_3^-
UDMH	89.55	3.85	0.30	6.30
NDMA	78.84	7.79	1.25	12.12
N_2H_4	92.16	0.06	0.10	7.68
NH_3	83.04	3.01	0.08	13.87

following interaction of obtained $NH_{2(ads)}$ particles with photogenerated $\dot{O}H_{(ads)}O^-_{2(ads)}$ and $O^-_{(ads)}$ species:

$$N_2H_{4(gas)} \rightarrow N_2H_{4(ads)} \rightarrow 2NH_{2(ads)} \tag{2.1}$$

$$NH_{2(ads)} + \dot{O}H_{(ads)} \rightarrow NH_{(ads)} + H_2O_{(ads)} \tag{2.2}$$

$$NH_{(ads)} + \dot{O}H_{(ads)} \rightarrow N_{(ads)} + H_2O_{(ads)} \tag{2.3}$$

$$NH_{(ads)} + O^-_{2(ads)} \rightarrow HNO_{(ads)} + O^-_{(ads)} \tag{2.4}$$

$$2N_{(ads)} \rightarrow N_{2(ads)} \rightarrow N_2\uparrow \tag{2.5}$$

$$N_{(ads)} + NO_{(ads)} \rightarrow N_2O_{(ads)} \rightarrow N_2O_{(g)}\uparrow \tag{2.6}$$

$$HNO_{(ads)} + \dot{O}H_{(ads)} \rightarrow NO_{(ads)} + H_2O_{(ads)} \tag{2.7}$$

$$NH_{2(ads)} + NO_{(ads)} \rightarrow N_{2(g)}\uparrow + H_2O_{(ads)} \tag{2.8}$$

$$NO_{(ads)} + O_2 \rightarrow NO_{2(ads)} + O_{(ads)} \tag{2.9}$$

$$NH_{2(ads)} + NO_{2(ads)} \rightarrow N_2O_{(ads)} + H_2O_{(ads)} \tag{2.10}$$

$$N_2O_{(ads)} \rightarrow N_{2(g)}\uparrow + O_{(ads)} \tag{2.11}$$

$$NO_{2(ads)} \xrightarrow{Ox} \text{nitrates} \tag{2.12}$$

A similar mechanism (stages (2.4)–(2.12)) was described by Cant and Cole for the PCO of NO and NH_3 on TiO_2 surfaces [20]. Authors demonstrated that the N_2 formation rate exceeded the one of N_2O for 4.5 times in PCO of NH_3 and also detected a small amount of nitrates. For PCO of UDMH, the main mechanistic features are as follows:

- molecular nitrogen (N_2) and adsorbed nitrates ($NO^-_{3(ads)}$) are the main N-containing products (see stages (2.5), (2.8), (2.11) and (2.12));
- the absorption band attributed to $N_2O_{(ads)}$ in the TiO_2 IR spectra testifies in favour of this species formation (stages (2.6) and (2.10));

The initial stages of PCO of UDMH and NDMA vapours probably proceed through the breakage of N–N bond:

$$(CH_3)_2NNO_{(ads)} \rightarrow (CH_3)_2N_{(ads)} + NO_{(ads)} \tag{3}$$

$$(CH_3)_2NNH_{2(ads)} \rightarrow (CH_3)_2N_{(ads)} + NH_{2(ads)} \tag{4}$$

The reaction (4) is known to occur in the gas phase under the thermal activation [21]. In PCO, the N–N bond breakage could be catalyzed by TiO_2 surface analogously to stage (2.1). The $NO_{(ads)}$ and $NH_{2(ads)}$ species could be directly involved into the processes described by stages (2.2)–(2.12). The transformation of $(CH_3)_2N$ species probably proceeds through the oxidation of CH_3 groups and formation of the NH and NH_2 particles on the one hand and formic acid and, further, CO_2 and H_2O, on the other hand.

Serpone and co-workers studied the titania-photocatalyzed oxidation of ethanolamines in aqueous solutions [22]. The authors demonstrated that hydroxyl radicals could attack amines either at the carbon atoms or the nitrogen atoms eventually leading to the formation of CO_2, NH_4^+ and a small amount of NO_3^-. In gas phase PCO, the formation of HNO_3 is more preferable than that of NH_3 probably due to a higher lability of adsorbed NH_3 molecule as compared to the symmetrical solvated NH_4^+ ion. Moreover, it will be demonstrated below that ammonium is oxidized into nitrates on the UV-irradiated TiO_2 surface.

According to the PCO mechanism equations (2.1)–(2.12) the formation of gaseous NO and NO_2 also probable but according to our FTIR measurements using Vector-22 (Bruker) spectrometer with low detection limit equal to 5 ppm for both gases they were not observed. Nevertheless if to recalculate the ratio of molecular N_2 taking into account the possible presence of NO_x in the gas phase then this ratio will become lesser in 2–3%.

3.4. Catalyst deactivation

In practice, the PCO N-containing products of UDMH should accumulate on the TiO_2 surface on course of long-term reaction. The deactivation of photocatalyst may develop due to the decrease of the number of surface sites available for the reaction in several consecutive batch runs over the photocatalyst.

The CO_2 evolvement and changes in TiO_2 surface spectra are shown in Fig. 7A and B, respectively. One can see that the UDMH conversion ultimate level remained unchanged at 85%, although the conversion time necessary to reach this level increased from 150 to 180 min. Since the product accumulating on the TiO_2 surface is nitric acid, the rising from run to run absorption bands 1316 and 1445 cm^{-1} in Fig. 7 are attributable to nitric acid (Fig. 5), one can make a conclusion that the photocatalyst activity remained almost unchanged as nitric acid accumulated on the surface.

To elucidate the effect of nitrate ion, the additional experiments were performed on the effect of adsorbed nitrates on the PCO rate of UDMH and acetone in the continuous flow reactor.

The reason of the acetone vapour PCO rate measurement in this work is that this reaction was well investigated previously [23,24]. H_2O and CO_2 was found to be the only end products of PCO. There were not detected any catalyst deactivation during acetone PCO and therefore this reaction is good test for the measuring of the TiO_2 photocatalyst activity [25].

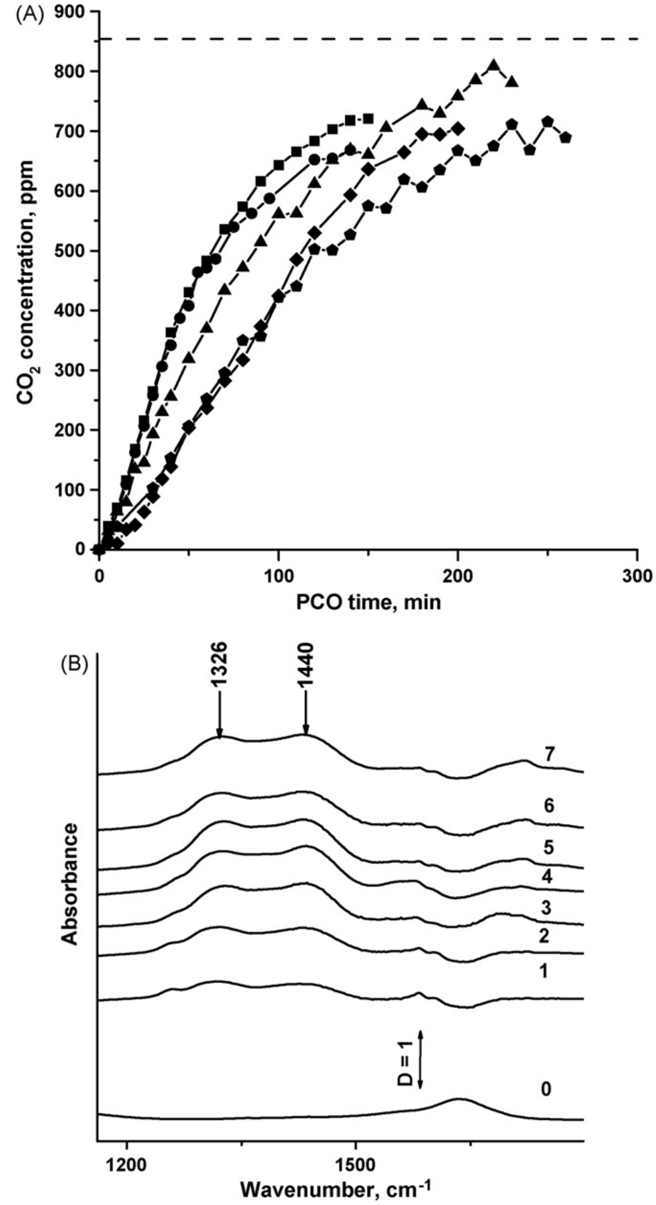

Fig. 7. PCO of seven consecutive runs of UDMH in the batch reactor: 300 K, the amount of UDMH 0.5 μl. (A) – Kinetics of the CO_2 evolvement in the gas phase. Symbols ■, ●, ▲, ◆, ⬟ correspond to 1st, 2nd, 4th, 5th and 6th run. Dashed line corresponds to the 100% UDMH conversion to gaseous CO_2. (B) – IR spectra of the TiO_2 surface after the PCO of each run. Spectrum (0) – pure TiO_2 sample, all other numbers above spectra correspond to the number of oxidation run. D – Absorbance.

For the experiment on the NO_3^- ions effect several samples of TiO_2 powder were impregnated with HNO_3 aqueous solution of different concentrations. The dependence of CO_2 formation rates for acetone and UDMH on the HNO_3 content were measured and are shown on the Fig. 8. One can see that the PCO rate of acetone was independent on the quantity of adsorbed HNO_3. The PCO rate of UDMH increased with the increase of the HNO_3 content. This increase could be attributed to two simultaneous tendencies: the increased adsorption of basic UDMH on the acidic photocatalyst, and the changes in adsorption and activation energies of some stages of complex PCO reactions due to the change of surface acidity [26]. One may conclude, therefore, that nitric acid may not be a direct reason for the catalyst deactivation.

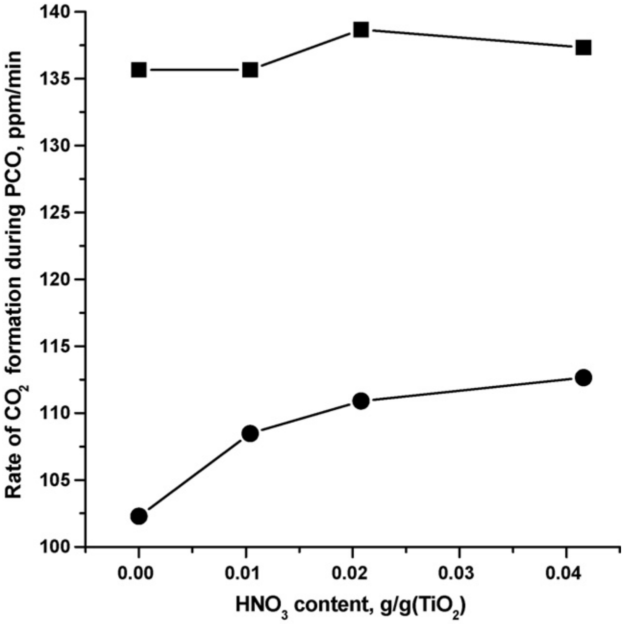

Fig. 8. Dependence of the rate of CO_2 formation in PCO of acetone (■) and UDMH (●) on the HNO_3 content on the photocatalyst surface in the continuous flow reactor: air flow 25 cm^3/min, humidity 50%, 300 K. Illumination by condensed light of Xe-lamp at 70 mW/cm^2.

Table 3
Quantity of ammonium and nitrate ions on the surface of TiO_2 impregnated with NH_4NO_3 salt before and after UV irradiation in the batch reactor (temperature T = 300K, humidity χ = 0%, illumination time t = 180 min, illumination was conducted by condensed light of high pressure Hg lamp, W = 20 mW/cm^2)

Ion	Quantity, 10^{-6} mole	
	Before irradiation	After 180 min of irradiation
NH_4^+	18.5	10
NO_3^-	18.5	23.8

The picture changed when NH_4NO_3 was used instead of HNO_3 for TiO_2 impregnation. The composition of nitrogen-containing species changed on course of UV-irradiation of the photocatalyst impregnated with ammonium nitrate in the batch reactor (see Table 3); a small amount of gaseous N_2O was also detected in the gas phase during the PCO experiment. The quantities of ammonium and nitrate ions, equal before irradiation, changed: after 180 min of irradiation, the quantity of NH_4^+ decreased by 10 μmole, whereas the NO_3^- quantity increased only by 5.3 μmoles. Thus, the residual nitrogen was evolved in the N_2 and N_2O forms and the N_2 quantity was bigger than the N_2O one. The following reaction pathway for the PCO of ammonium nitrate could be proposed:

$$NH_4NO_3 \xrightarrow{h\nu, TiO_2} N_2O + H_2O + HNO_3 + N_2$$

4. Conclusions

1. Photocatalytic oxidation of UDMH proceeds until complete mineralization of the target compound in a batch reactor with carbon dioxide, surface nitrates, ammonium and molecular nitrogen as the major final products.
2. N_2O was registered as the surface and gaseous intermediate product in the PCO of UDMH.
3. Similar behaviour of N_2H_4, $(CH_3)_2NNO$ and $(CH_3)_2NNH_2$ in PCO was observed with surface nitrates and ammonium, and gaseous nitrogen being the major N-containing ultimate products, and N_2O being the minor gaseous and surface intermediate.
4. Accumulation of surface nitrates in the long-term PCO of UDMH was responsible for the TiO_2 photocatalyst insignificant deactivation, which was explained by the minor, about 10%, amount of initial UDMH nitrogen converted to the surface nitrates and the major amount of nitrogen evolved in the molecular nitrogen form.
5. Universal mechanism is proposed to explain the kinetic features and products distribution of hydrazine and its derivatives, nitrosodimethylamine and dimethylhidrazine.

Acknowledgement

This work was financially supported by the NATO (''Science for Piece'', grant 981461) and the Academy of Sciences of Finland (Program ''Russia in flux'', grant 208134).

References

[1] H.W. Shiessl, Fourth ed., Hydrazine and its Derivatives, Kirk-Othmer Encyclopaedia of Chemical Technology, vol. 13, John Wiley & Cons Inc., 1995, pp. 560–606.
[2] I.Z. Ismagilov, V.V. Kuznetsov, A.P. Nemudryi, O.Y. Pod'yacheva, Kinet. Catal. 45 (5) (2004) 722.
[3] O.P. Pestunova, G.L. Elizarova, M.A. Kerzhentsev, V.N. Parmon, Catal. Today 75 (2002) 219.
[4] Z.R. Ismagilov, M.A. Kerzhentsev, I.Z. Ismagilov, V.A. Sazonov, V.N. Parmon, G.L. Elozarova, O.P. Pestunova, V.A. Shandakov, Y.L. Zuev, V.N. Eryomin, N.V. Pestereva, F. Garin, H.J. Veringa, Catal. Today 75 (2002) 277.
[5] K. Utvary, G. Vitovec, R. Kren, H.H. Sisler, Moratsh. Chem. 103 (11) (1972) 239–242.
[6] K. Utvary, H.H. Sisler, Inorg. Chem. 7 (14) (1968) 698–701.
[7] W.A. Mitch, J.O. Sharp, R.L. Valentine, L. Alvarez-Cohen, D.L. Sedlak, Environ. Eng. Sci. 20 (2003) 389.
[8] M.I. Schreiber, W. Mitch, Influence of the order of reagent addition on NDMA formation during chloramination, Environ. Sci. Technol. 39 (2005) 389.
[9] J.G. Aston, J.L. Wood, T.P. Zolki, J. Am. Chem. Soc. 75 (1953) 6202.
[10] Problem aspects of utilization methodology of composite solid rocket propellants, scrap propellants and liquid rocket propellant residue in the elements of rocket-space technics, Federal research & Production Center ALTAI, Russian Rocets & Artillery Academy, Biisk, 2003.
[11] W.H. Strehlow, E.L. Cook, J. Phys. Chem. Ref. Data 2 (1) (1979) 163.
[12] H.E. Malone, D.M.W. Anderson, Anal. Chim. Acta 48 (1969) 87.
[13] A.A. Davidov, IR-spectroscopy in chemistry of surface oxides. Novosibirsk, Science (1984) 44.
[14] R. James, Durig, C. Zheng, Vib. Spectrosc. 30 (2002) 59.
[15] D.V. Kozlov, A.V. Vorontsov, P.G. Smirniotis, E.N. Savinov, Appl. Catal. B 42 (2003) 77.
[16] Coblentz Society, Inc., ''Evaluated Infrared Reference Spectra'' in NIST Chemistry WebBook, NIST Standard Reference Database Number 69, P.J. Linstrom, W.G. Mallard (Eds.), National Institute of Standards and Technology, Gaithersburg MD, June 2005, 20899 (http://webbook.nist.gov).
[17] O.M. Alfano, M.I. Cabrera, A.E. Cassano, J. Catal. 172 (1997) 370.
[18] C.S. Turchi, D.F. Ollis, J. Catal. 122 (1990) 178.
[19] C. Chuang, J. Shiu, J. Lin, Phys. Chem. Chem. Phys. 2 (2000) 2629.
[20] N.W. Cant, J.R. Cole, J. Catal. 134 (1992) 317.
[21] H.F. Cordes, J. Phys. Chem. 65 (1961) 1473.
[22] S. Horikoshi, N. Watanabe, M. Mukae, H. Hidaka, N. Serpone, New J. Chem. 25 (2001) 999.
[23] A.V. Vorontsov, E.N. Savinov, G.B. Barannik, V.N. Troitsky, V.N. Parmon, Catal. Today 39 (1997) 207.
[24] A.V. Vorontsov, E.N. Savinov, P.G. Smirniotis, Chem. Eng. Sci. 55 (2000) 5089.
[25] D. Kozlov, D. Bavykin, E. Savinov, Catal. Lett. 86 (2003) 169.
[26] D.V. Kozlov, A.A. Panchenko, D.V. Bavykin, E.N. Savinov, P.G. Smirniotis, Russ. Chem. Bull., Int. Ed. 5 (2003) 1100.